Really Large Hadron Colliders*

G. Dugan
Cornell University, Ithaca, NY 14853

ABSTRACT

This paper presents two possible approaches to a post-LHC hadron collider. The parameters and some of the accelerator physics issues of the two designs are discussed, followed by comments on the challenges involved in the technical systems. Major issues for further study and R&D are listed in the conclusion.

I. INTRODUCTION

In this paper, a “really large” hadron collider will be taken to mean a proton-proton collider with a center-of mass energy in excess of 60 TeV. This machine is envisioned to be a successor to the CERN Large Hadron Collider (14 TeV center-of-mass energy), which is currently planned to be completed in the middle of the next decade.

Such an accelerator has several general characteristics. The most important of these is that this machine will be on the energy frontier. There is no currently feasible high-energy accelerator technology other than a proton-proton collider which can access these energies.

The very high energy of the machine requires that it have a large size (hence the name “really large”). There are several consequences of this large size. First, the machine will cost a lot of money to build and to operate. This is the driving force behind the efforts described below to minimize the cost as much as possible. The large cost means that the construction effort will stretch over many years (since in general political processes limit the amount of money per year available for construction). The long construction effort requires very detailed planning efforts and the necessity of maintaining support for the project over long time periods.

The use of resistive magnets in such a large machine would result in prohibitively large operating costs. Hence, the use of superconducting magnets is mandatory. The ability to develop high fields in such magnets provides an additional benefit by limiting the circumference of the machine (for a fixed energy) and hence the amount of civil construction required for the subterranean tunnels. Nevertheless, the machine will still require many tens to hundreds of kilometers of such tunnels. Because of the repetitive nature of the accelerator lattice, the tunnels will be filled with many copies of the same component. The production of the accelerator’s components thus has a strong “mass production” flavor, and generally must involve the use of production engineering techniques and the involvement of industries experienced in such techniques.

*Work supported by the National Science Foundation

Finally, the enormous investment of time and resources demands that, although the accelerator will be at the state-of-the-art, its basic design must be sufficiently conservative that it will operate reliably for high-energy physics at its design parameters soon after initial commissioning.

II. PROPOSALS TO BE STUDIED AT THIS WORKSHOP

Two different approaches to a “really large hadron collider” (RLHC) will be studied at this workshop. These two approaches have three common features:

• Both approaches aim to provide a "discovery machine" on the energy frontier in the post-LHC era(>2010). Specifically, both will provide machines with a center-of-mass energy in excess of 60 TeV and a luminosity in excess of $10^{34}cm^{-2}sec^{-1}$.

• Both approaches strive to be "affordable”. They do not propose simply to duplicate the technology of the LHC or SSC on a larger scale, which is generally perceived as being excessively expensive and unable to obtain the necessary support. Instead, they use new ideas and new technologies which are intended to reduce the cost per TeV substantially below that of LHC or SSC. The successful implementation of such new ideas and technologies to reduce cost is crucial to the effort.

• In both approaches to the RHLC, some elements of the required new technology are beyond the current state-of-the-art. Given the extended time between the present and the possible construction start (>2010), such technological extrapolations are not considered to be a serious defect in the proposals. They are the focus of future R&D efforts.

A. High-field approach

The basic idea for this approach was first developed at the 1994 DPF/DPB Indiana Workshop[1]. The essence of the approach is to choose the parameters of the machine so that the synchrotron radiation damping time at full energy is significantly shorter than the mean store duration[2]. The radiation damping then provides substantial relief from one of the major problems in hadron colliders, the requirement for emittance preservation. Relief from this requirement means reduced magnetic field quality requirements at injection (which means less difficult magnets), and a less demanding, and consequently simpler, injector complex.

The radiation damping time for the horizontal amplitude in a proton-proton collider is given by

$$\tau_x = \frac{2\tau_0}{1-D}, \quad (1)$$

in which the characteristic time τ_0 is

$$\tau_0 = \frac{E}{f_0 \Delta E}, \quad (2)$$

and

$$\Delta E = \gamma^4 m_p c^2 \frac{4\pi r_p}{3\rho} \quad (3)$$

is the energy lost per turn due to synchrotron radiation. In eq. (1), for a separated function lattice with a transition gamma γ_t,

$$D = \frac{1}{\gamma_t^2}$$

is small compared to 1. For a combined function lattice, however, D can be greater than 1, producing horizontal antidamping.

The other variables in the above equations are the revolution frequency

$$f_0 = \frac{cg}{2\pi\rho} = \frac{c}{C}, \quad (4)$$

the filling factor

$$g = \frac{2\pi\rho}{C}, \quad (5)$$

and the bending radius in the dipoles

$$\rho = \frac{E}{eBc}. \quad (6)$$

B is the magnetic field in the dipoles, C is the ring circumference, the rest energy of the proton is $m_p c^2$=0.938 GeV, and the classical proton radius is

$$r_p = \frac{e^2}{4\pi\varepsilon_0 m_p} = 1.533 \times 10^{-18} \text{ m}. \quad (7)$$

The beam energy is E, and $\gamma = \frac{E}{m_p c^2}$. We can obtain a relation for τ_0 in terms of γ and B by combining equations (2), (3), (4), (6) and (7) to get

$$\tau_0 = \frac{E}{f_0 \Delta E} = \frac{3\rho^2}{2g\gamma^3 c r_p} = \frac{3m_p^2 c}{2r_p e^2} \frac{1}{gB^2\gamma}. \quad (8)$$

For a beam energy of 30 TeV, fig. 1 shows the characteristic damping time vs. dipole field (for g=0.8). To achieve characteristic damping times of less than 2 hr, (which lead to amplitude damping times less than 4 hr for separated function lattices), dipole fields of above 12 T are required.

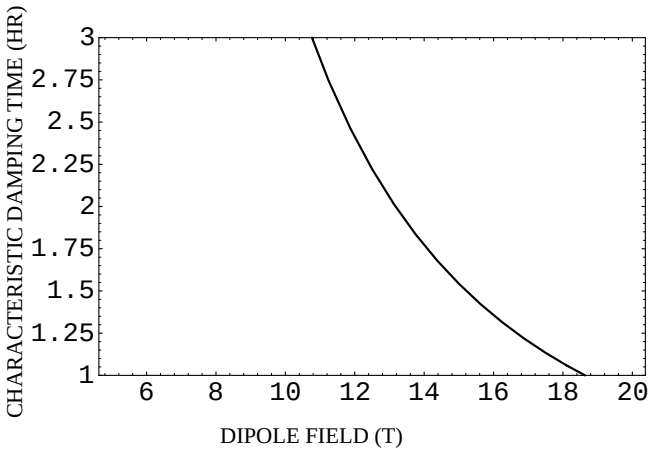

FIG. 1: Characteristic damping time vs. dipole field

The circumference of such a ring is given from eqs. (5) and (6) as

$$C = \frac{2\pi E}{egBc} = \frac{2\pi m_p c}{e} \frac{\gamma}{gB}. \quad (9)$$

For a 12.5 T dipole field, a 30 TeV ring with g=0.8 has a circumference of about 62 km.

Because of the high field and consequently the relatively small circumference (about 2/3 the SSC circumference, with 3/2 the energy), such an approach has the potential for reduced civil costs. On the other hand, the development of cost effective 12.5 T magnets is a real challenge. Such magnets are beyond the reach of existing NbTi technology; they will require at least the use of such materials as Nb_3Sn. The preferable approach, if the technology will support it, would be the use of high temperature superconducting (HTS) materials in the 15-20^{O}K range

B. Low-field approach

The ideas used in this approach have been developed primarily at Fermilab[3] and have been discussed in symposia at the 1996 Indianapolis APS meeting[4]. The essence of the approach is to use a very simple, novel, 2-in-1 combined function superferric magnet, which would operate with a field of less than 2 T. This magnet, called the "double-C transmission line magnet", offers the possibility of dramatically reduced magnet system costs due to its simplicity and ease of construction.

On the other hand, the low field requires that the ring circumference be large (from eq. (9) above, a 30 TeV 1.8 T low-field ring has a 390 km circumference). For this to be affordable, one must develop and implement very-low-cost innovative tunneling and installation technologies. The suggestion of simply housing the accelerator in a pipe buried under the ground has led to the name "Pipetron" for this approach.

III. PARAMETERS AND ACCELERATOR PHYSICS ISSUES

In this section, I will present the parameters of several design examples in order to illustrate some of the accelerator physics issues. I will compare parameters for the low field and high field approaches for a 30 TeV/beam ring. Since a very high energy alternative has also been discussed for the low-field approach [4], I also present the parameters for a 100 TeV/beam low field ring. For reference, I include in each parameter table the values for the LHC ring. The designs shown are taken partially from previous work[1,2,3,4], but are not necessarily optimized, and for the LHC may not correspond exactly to the current design. Hence the parameters should be viewed only as illustrative.

A. Luminosity Parameters

Table I: Luminosity parameters

Parameter	LHC	High field	Low Field A	Low field B	Units
CM Energy	14	60	60	200	TeV
Dipole field	8.4	12.6	1.8	1.8	T
Circumference	26.7	62.3	388	1300	km
Synchrotron radiation damping time	51.2	4.4	189.2	57.3	hr
Initial luminosity	1	.35	1	1	10^{34} $cm^{-2}sec^{-1}$
Rms normalized emittance	3.75	1.5	1.5	1.5	π μm-rad
β^*	.5	.2	.2	.2	m
Protons/bunch	9.5	2.1	2.8	1.6	10^{10}
Number of bunches	3570	2090	22880	76650	
Equilibrium emittance (x)	.45	23.8	.23	1.8	10^{-3} π μm-rad

The initial luminosity given in table I is calculated from

$$L = \frac{\gamma}{4\pi\varepsilon_n\beta^*} f_0 B_n N_B^2 R(\alpha, \sigma_s, \gamma, \varepsilon_n\beta^*) = \frac{\gamma}{4\pi\varepsilon_n\beta^*}\frac{N_B^2}{S_B} R(\alpha, \sigma_s, \gamma, \varepsilon_n\beta^*) \quad , \qquad (10)$$

in which N_B is the number of protons per bunch in each beam (assumed equal); S_B is the bunch spacing; ε_n is the rms normalized emittance (assuming round beams); β^* is the beta function at the interaction point; and R is a function in the range of 0.8 to 0.9, which represents the luminosity reduction due to both a finite crossing angle and the "hourglass effect" (reduction due to the variation of the beta function over the bunch length). The values assumed for N_B, ε_n, β^*, and B_n, the number of bunches, are given in table I; the bunch spacing is

$$S_B = \frac{C}{B_n} \quad . \qquad (11)$$

The values shown in table I for the numbers of protons per bunch and the rms emittances are within the capabilities of a conventional injector complex (although great care must be taken in emittance preservation in the injector chain to achieve these values).

The initial luminosity for the high field case is well below $10^{34}cm^{-2}sec^{-1}$, but because of the radiation damping, it increases during the store, peaking near $10^{34}cm^{-2}sec^{-1}$, after a few hours. This behavior is illustrated in fig. 2, which shows the evolution of the luminosity during a store, for both the high field and low field (30 TeV) examples. (In this figure, only radiation damping and particle loss due to collisions at the interaction points are considered; intrabeam scattering is neglected. The inclusion of intrabeam scattering changes the details of the high field time evolution but the general picture remains the same.)

Two curves are shown in fig. 2 for each case: one for an initial rms normalized emittance of 1π μm-rad, and one for 2π μm-rad. In the latter case, the luminosity is reduced for the low field case by a factor of two at all times; but for the high field case, there is a reduction only at early times in the store; after about 5 hours, radiation damping entirely determines the emittance and the luminosity is quite independent of the initial emittance. This feature is the major selling point of the high field design. It makes the integrated luminosity performance of this design relatively insensitive to the initial emittance. The consequence of this is much greater tolerance to emittance dilution in the injector chain. There is also greater tolerance to emittance growth in the collider itself at injection energy, and consequently greater tolerance to magnet manufacturing and installation errors.

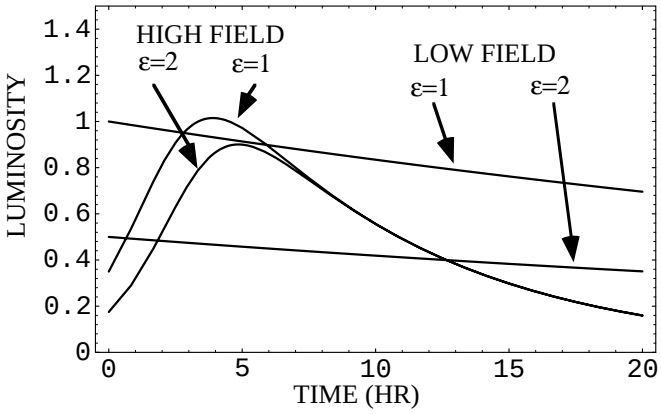

FIG. 2: Time evolution of the luminosity (in $10^{34}cm^{-2}sec^{-1}$). Emittances are given in π μm-rad.

B. Energy/power parameters

Table II illustrates the stored energy in the beam for each case

$$E_{store} = N_T E, \tag{12}$$

and the total power in synchrotron radiation per ring

$$P_s = f_0 \Delta E N_T = \frac{2ec^2}{3\varepsilon_0}\frac{\gamma^4 I}{gC}, \tag{13}$$

in which I is the total beam current

$$I = \frac{ecN_T}{C}, \tag{14}$$

and N_T is the total number of protons

$$N_T = C\frac{N_B}{S_B}. \tag{15}$$

Table II: Energy/power parameters

Parameter	LHC	High field	Low Field A	Low field B	Units
CM Energy	14	60	60	200	TeV
Bunch spacing	25	100	57	57	nsec
Beam stored energy	.377	.212	3.04	19	GJ
Synchrotron radiation power/ring	4.1	27	8.9	184	kW
Total protons/ring	3.37	.44	6.34	11.88	10^{14}

From eq. (10), the luminosity

$$L \propto \frac{N_B^2}{S_B} = \frac{N_T^2 S_B}{C} \tag{16}$$

can remain constant as the number of particles N_T is reduced if the bunch spacing increases. For the high field case, it is important to limit the synchrotron radiation power, because it is delivered to a cold surface (probably a beam screen; see sect. IV.C below) and hence costs refrigeration power. The synchrotron radiation power is limited by using a small value for N_T which requires a large bunch spacing. The small value of N_T also leads to a rather small beam stored energy for the high field case (less than for the LHC).

The synchrotron radiation power is less important for the low field case, which has a warm beam pipe (see sect. IV.C below). However, as eq. (16) shows, because of the large circumference, the low field case inevitably requires a large value of N_T for a given luminosity, and the beam stored energy becomes enormous, as noted in table II. This will make abort design and the handling of single point beam loss severe problems for such a machine.

C. Collision point parameters (2 interaction regions)

Table III presents $\langle n \rangle$, the number of interactions per crossing expected for each design, computed from

$$\langle n \rangle = L\sigma_{int} S_B.$$

The choice of a large bunch spacing noted in the previous section inevitably leads to large numbers of interactions per crossing. This, of course, creates a relatively inhospitable environment at the collision point and puts severe pressure on the detector design. Reduced bunch spacing, for fixed luminosity, leads to fewer interactions per crossing but increases the beam stored energy and the synchrotron radiation power, as discussed in the previous section. A crucial machine/detector interface issue is the proper tradeoff between detector problems related to large numbers of interactions per crossing and the accelerator systems issues required to cope with large beam stored energy and large amounts of synchrotron radiation power.

Table III: Collision point parameters (2 Interaction regions)

Parameter	LHC	High field	Low Field A	Low field B	Units
CM Energy	14	60	60	200	TeV
Interactions /crossing	19	38	61	83	
Beam lifetime (pp collisions only)	60	16	80	110	hr
$\sigma_{inelastic}$	78	110	110	150	mbarn

Also shown in table III is the beam lifetime due to pp interactions at the 2 interaction points

$$\tau_{pp} = \frac{N_T}{2L\sigma_{int}}. \tag{17}$$

To limit the synchrotron radiation power, the high field design works with a small number of particles, as noted in the previous section; besides giving a large number of interactions per crossing, this choice also leads to a relatively short beam lifetime due to pp collisions. The stores in this machine will consequently need to be "short" (probably under 10 hours). The injector must fill relatively quickly, which is not a problem for a small diameter ring (see sect. E below).

D. Interaction point/beam-beam parameters

Table IV gives the parameters associated with the beam-beam interactions which occur in the vicinity of the interaction point(IP). The total head-on tune shift, $\Delta\nu_{HO}$, is given by

$$\Delta\nu_{HO} = \frac{2N_B r_p}{4\pi\varepsilon_n} \tag{18}$$

for round beams and two interaction regions. The total long-range tune shift, $\Delta\nu_{LR}$, is

$$\Delta\nu_{LR} = \frac{r_p N_B n_{LR}}{2\pi\gamma\alpha^2\beta^*}, \tag{19}$$

in which n_{LR} is the number of long-range crossings

$$n_{LR} = \frac{2L_{LR}}{S_B}, \tag{20}$$

and L_{LR} is the distance over which long-range interactions occur (the distance from the IP to the beam separation dipole).

Table IV: Interaction point/beam-beam parameters

Parameter	LHC	High field	Low Field A	Low field B	Units
CM Energy	14	60	60	200	TeV
Rms bunch length at interaction point	7.5	4	5	5	cm
Initial rms beam size at interaction point	16	3	3.1	1.7	μm
Crossing full-angle	200	50	50	35	μrad
Rms normalized emittance	3.75	1.5	1.5	1.5	π μm-rad
$\frac{\gamma\alpha^2\sigma_s^2}{4\beta^*\varepsilon_n}$	.22	.11	.17	.27	
R	.88	.91	.87	.83	
$\Delta\nu_{HO}$ (total, head-on)	6	3.4	4.4	2.5	10^{-3}
IP to separation dipole length	50	100	70	200	m
$\Delta\nu_{LR}$ (total, long-range)	4	4.2	6.8	6.7	10^{-3}
Δν (total)	10	7.6	11.3	9	10^{-3}

As table IV shows, the total beam-beam tune shift

$$\Delta\nu = \Delta\nu_{LR} + \Delta\nu_{HO} \tag{21}$$

for all designs is initially in the (conservative) range of 0.01. However, as the high-field beam size shrinks during the store, the head-on beam-beam tune shift increases by as much as a factor of two, bringing it closer to the limiting value of 0.025 experienced in existing proton-antiproton colliders. In addition, it is worth noting that the small beam size for the high-field case at peak luminosity, and for the low field case B initially, means that these cases will have the most sensitivity to luminosity loss due to vibration.

Also shown in table IV is the luminosity reduction factor R arising from the finite crossing angle and variation of the beta function over the bunch length:

$$R \cong \frac{1}{\sqrt{1+\frac{\gamma\alpha^2\sigma_s^2}{4\beta^*\varepsilon_n}}}\left[1-\left[\frac{\sigma_s}{\beta^*}\right]^2\right]. \tag{22}$$

All the designs are constrained to keep $\frac{\gamma\alpha^2\sigma_s^2}{4\beta^*\varepsilon_n}$ small compared to 1 (to prevent loss of luminosity) while at the same time keeping $\Delta\nu_{LR}$ small. In practice, this can only be done by keeping the rms bunch length at collision, σ_s, in the 5 cm range.

E. Longitudinal parameters (in collision)

Table V: Longitudinal parameters (in collision)

Parameter	LHC	High field	Low Field A	Low field B	Units
CM Energy	14	60	60	200	TeV
Revolution frequency	11.2	4.8	.77	.23	kHz
Synchrotron frequency	20.3	9.8	.59	.14	Hz
Rf Voltage	18	50	25	50	MV
Rms longitudinal bunch area	.78	.52	1.0	2.3	eV-sec
α_p: Slip factor	2.2	2.2	.10	.03	10^{-4}
Harmonic number	3.564	8.4	52	174	10^4
Radio-frequency	400	403	402	402	Mhz
Energy loss/turn	6.8	792	113	4189	keV
Bucket area	10	24	31	73	eV-sec
Rms bunch length at IP	7.5	4	5	5	cm
Rms relative energy spread	142	42	68	49	10^{-6}

In table V, I present the parameters associated with the longitudinal degree of freedom of the beam. In all the relations given below, I take β =1, assume that the beam is far above transition

$$\gamma >> \gamma_t = \frac{1}{\sqrt{\alpha_p}}$$

(in which α_p is the momentum compaction), and take the synchronous phase to be zero. Then the synchrotron frequency is given by

$$f_s = \frac{c}{C}\sqrt{\frac{eV_{RF}h\alpha_p}{2\pi E}}, \tag{23}$$

in which h is the harmonic number and V_{RF} is the rf voltage. As table V shows, because of their large radius, the low field

designs have very low revolution and synchrotron frequencies-below 1 Hz. Ground and environmental vibration power spectra grow very large at such low frequencies, and will be a major source of concern for emittance growth in the low field designs.

In collision, with a longitudinal bunch area ε_l, the bunch length is given by

$$\sigma_s = c\sqrt{\frac{\varepsilon_l}{\pi f_0}}\sqrt{\frac{\alpha_p}{2\pi EeV_{RF}h}}. \qquad (24)$$

With rf frequencies in the range of 400 MHz (a practical choice, but not absolutely required), all designs need relatively large rf voltages to keep the bunch length in the 5 cm range.

It appears from eq. (24) that a reduced longitudinal bunch area would reduce the bunch length without the need for a large rf voltage. However, in the low field case, reducing the longitudinal bunch area to reduce the bunch length would also reduce the momentum spread, since

$$\sigma_p = \sqrt{\frac{\varepsilon_l f_0}{\pi}}\sqrt{\frac{2\pi EeV_{RF}h}{\alpha_p}}. \qquad (25)$$

Since the low field designs are on the edge of longitudinal stability already (see below, section F), the momentum spread cannot be reduced. In the high field design, a relatively large longitudinal bunch area is also needed to suppress intrabeam scattering. In fact, because in this case radiation damping alone will reduce the longitudinal area to an unacceptably low level, an artificial means for heating the beam longitudinally during the store will be required.

E. Injection parameters

Table VI: Injection parameters

Parameter	LHC	High field	Low Field A	Low field B	Units
CM Energy	14	60	60	200	TeV
Fill time		6.5	16.3	34.7	min
Acceleration time	2.6	10.4	26	144	min
Total time: fill and accelerate		17	42	179	min
LEB	1.4	8	8	150	GeV
MEB	26	150	150	1000	GeV
HEB	.45	1	1	5	TeV
Injection/full energy	6.4	3.3	3.3	5	%
Rf acc. voltage	8	20	50	100	MV

Table VI presents some parameters associated with injection. The specified injector chains are chosen so that the ratio of injection energy to full energy is always at least 3%. This may be marginal for the low field case; for the high field case, the benefits of radiation damping at full energy may make this choice workable.

The fill times shown assume coalescing at flattop in at least one of the injectors. They assume an acceleration rate a = 30 sec/TeV in the last injector (which is taken to be a superconducting accelerator), and assume that the line density in this injector is l=3.3x10^{12} particles per kilometer. Then the filling time is given by

$$\tau_{fill} = \frac{N_T}{N_{inj}}\tau_{inj}, \qquad (26)$$

in which the injector cycle time is

$$\tau_{inj} = 2aE_{inj}, \qquad (27)$$

and the number of particles in the injector is

$$N_{inj} = C_{inj}l. \qquad (28)$$

Combing eqs. (26)-(28) leads to

$$\tau_{fill} = \frac{2aN_T}{l}\frac{g_{inj}ecB_{inj}}{2\pi}, \qquad (29)$$

which shows that the fill time depends linearly on the magnetic field in the (last) injector. The values given in table VI correspond to an injector with a field equal to that of the collider in each case.

The acceleration time in the collider is computed from the rf voltage shown, assuming a synchronous phase of 30^o:

$$\tau_{acc} = \frac{2E}{f_0 V_{RF}}. \qquad (30$$

Perusal of Table VI reveals that, because of the large number of particles and low revolution frequency in the low field designs, these machines take quite a while to fill and ramp.

F. Coherent stability parameters

Table VII illustrates several quantities related to beam stability. The second row shows the threshold for the single-bunch longitudinal microwave instability, calculated from the Keil-Schnell criterion as

$$\frac{Z_{||}}{n} = \frac{2\pi E\alpha_p\left(\frac{\sigma_p}{p}\right)^2}{eI_p}, \qquad (26)$$

in which the peak current, $I_{p,}$ is

$$I_p = \frac{eN_B c}{\sqrt{2\pi}\sigma_s}. \qquad (27)$$

For the low field cases, because of the small momentum compaction, the threshold is below one ohm, which is uncomfortably low. Care will be required in component design to be able to realize a large ring with such a small longitudinal impedance.

For these machines, the single bunch transverse mode-coupling instability (sometime referred to as the "fast head-tail") has the lowest transverse impedance threshold, given by

$$Z_{\perp} = \frac{4\pi\sqrt{2}E_{inj} f_s}{eI_p f_0 \langle\beta\rangle}. \qquad (28)$$

Table VII: Coherent stability parameters

Parameter	LHC	High field	Low Field A	Low field B	Units
CM Energy	14	60	60	200	TeV
Longitudinal impedance threshold: $\frac{Z_{\|\|}}{n}$(collision)	8.3	6.7	0.8	0.9	Ω
Transverse impedance threshold: $Z_{\perp}$(injection)	42	189	63	175	MΩ/m
Resistive-wall transverse impedance: $Z_{RW}(\frac{c}{\sigma_s})$ (injection)	0.1	0.4	160	510	MΩ/m
Resistive-wall multibunch instability growth time	329	926	.26	.18	turns
Total current	.6	.03	.09	.05	Amp
Peak current(inj)	14	4.9	9.3	5.8	Amp
<β>	64	140	191	382	m
Beam pipe radius	2.0	1.65	.75	.75	cm
Beam pipe	Cold, Cu	Cold, Cu	Warm, Al	Warm, Al	

As shown in table VII, all the designs have similar values for the threshold of this instability. However, the resistive wall impedance is very large in the low field machines, because of the large circumference and warm, small radius beam pipe. The resistive wall impedance at frequency ω is

$$Z_{RW}(\omega) = \frac{CZ_0}{2\pi b^3}\sqrt{\frac{2\rho}{\mu_0\omega}}, \qquad (29)$$

in which Z_0=377 Ω is the impedance of free space, b is the inside radius of the vacuum chamber, and ρ is the resistivity of the vacuum chamber material. The thickness of the vacuum chamber wall is assumed to be much greater than the skin depth at frequency ω. The resistive wall impedance, evaluated at a frequency $\omega=c/\sigma_s$ characteristic of the bunch, is shown in table VII. For the low field machines, this number is greater than the mode-coupling instability threshold, implying that the beam will be transversely unstable. Since such a high-frequency, single bunch instability is very difficult to damp, the only real recourse is to reduce the resistive-wall impedance given in eq. (29), for example by increasing the beam pipe radius.

The resistive wall impedance grows very large at low frequencies, and can drive multibunch instabilities. The growth time, in turns, for the resistive-wall driven transverse multibunch instability is

$$\tau_{wall} = \frac{4\pi b^3 E_{inj}}{e^2\langle\beta\rangle N_T c}\sqrt{\frac{\pi\Delta Q}{c\mu_0\rho C}}, \qquad (30)$$

in which we take $\Delta Q = n - Q \approx 0.1$. (This result is for a wall thickness much greater than a skin depth. Since this condition is usually not satisfied at the low frequencies associated with the multibunch instability, eq. (30) overestimates the growth time.) Table VII shows the growth times for the several machines. The low field machines, because of their small beam pipe radius, but large resistivity, circumference, and number of particles, have very short growth times-less than one turn. Active damping in this case will require a challenging feedback system.

G. Lattice/Dynamic Aperture

Table VIII: Parameters of the lattice

Parameter	LHC	High field	Low Field A	Low field B	Units
CM Energy	14	60	60	200	TeV
Half-cell length	50	110	150	300	m
Betatron beam size	1.1	.73	.85	.62	mm
Dispersion beam size	1.02	1.01	.6	.37	mm
10-sigma total beam size	15.4	12.5	10.4	6.5	mm
Beam pipe radius	20	16.5	7.5	7.5	mm

In table VIII, for specific choices of half-cell lengths $\hat{L}$, I show the maximum rms betatron beam size at injection

$$\sigma_\beta = \sqrt{\frac{\varepsilon_n \hat{L}}{3.41\gamma_{inj}}}, \qquad (31)$$

and the maximum beam size due to dispersion

$$\sigma_D = \frac{17\hat{L}^2}{C}\left[\frac{\sigma_p}{p}\right]_{inj}, \qquad (32)$$

for 90° cells. Also shown is the 10-sigma total beam size

$$\sigma_{10} = 10\sqrt{\sigma_\beta^2 + \sigma_D^2}\,. \tag{33}$$

This number exceeds the beam pipe radius for the low field case A, implying that a larger beam pipe, or a smaller half-cell length, would be needed. In general, longer cells are cheaper and may allow a sparser, simpler, cheaper correction system. However, as the equations above demonstrate, longer cells lead to larger beam sizes and so require larger apertures and /or a high injection energy. The aperture/cell length/injector tradeoff problem becomes much more complex when one considers the fact that the aperture of concern is usually not the beam pipe radius, but rather the dynamic aperture determined by error fields and magnet alignment.

H. Interaction Region

The design of the interaction region is a difficult problem which is common to, and similar in, both the high field and low field cases. An example design[5] at 30 TeV has β^* = 10 cm, with β_{max}= 40 km. Although it requires a formidable 300 T/m triplet, the beam size in the triplet is only 1.2 mm (σ) and so may allow quite small bore quads.

There are many other challenges in the design of the interaction regions. Among these are local coupling and chromatic control; issues of energy deposition in the quadrupole triplets; and alignment and vibration tolerances in the triplets.

IV. ACCELERATOR SYSTEMS

A. Magnets

For both the low and high field designs, the most costly system in the accelerator is that of the magnets. Consequently, both approaches strive for smaller, cheaper, and simpler magnets for affordability. However, because of the large difference in the choice of working field, the details are vastly different.

1. Low field

The magnet concept in this approach has been quite well developed at Fermilab[3]. It features a strikingly simple, low cost superferric (1.5-2T) combined function dipole called the “double-C transmission line” magnet. (See fig. 3)

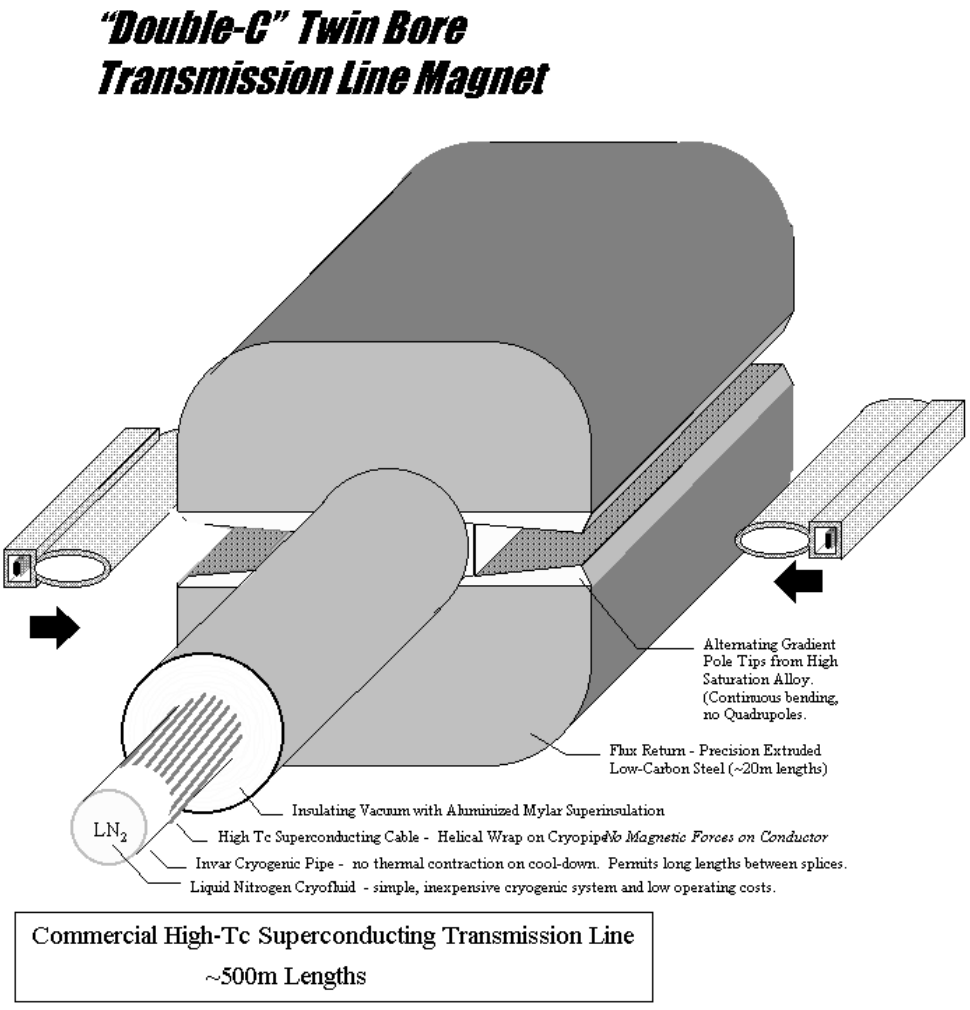

FIG. 3: Double-C transmission line magnet[3]

The magnet drive current is provided by a cylindrical conductor carrying 60 kA of supercurrent; this conductor is surrounded by an iron yoke, as shown in fig. 3, in such a way as naturally to provide a double bore magnet suitable for a proton-proton collider. The conductor is very similar to those used in superconducting transmission lines, and ideally would be fabricated from high temperature superconductor helically wrapped on the cryopipe. It could also be made from conventional NbTi conductor. The location of the conductor at a force null eases many of the mechanical design and heat leak problems. The poles are shaped to provide a gradient as well as a dipole field, which makes the machine combined-function. Field quality is achieved by shaping the iron pole tips.

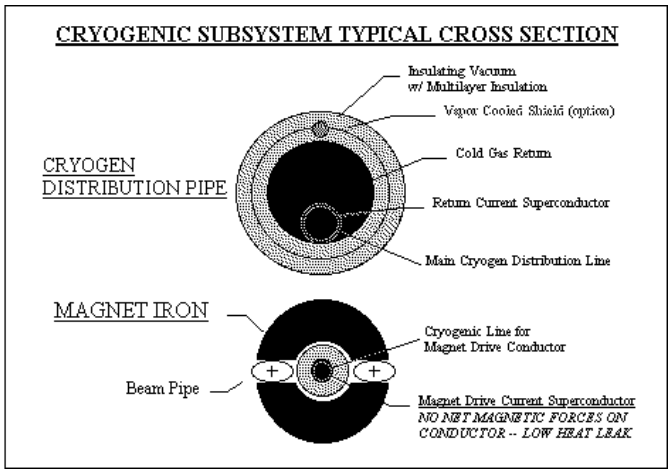

FIG. 4: Cryogenic return system for double-C magnet[3]

The current is returned in another cryostat located above the double-C magnet, as shown in fig. 4. The vacuum chamber, shown in fig. 3, is warm aluminum, with antechambers for pumping the gas generated by the beam's synchrotron radiation.

One of the principal goals of the magnet design is to achieve 10x lower magnet cost per TeV than conventional high-field superconducting magnets. The simplicity of the design, the sparing use of superconductor (10x less than in a cos θ dipole), and the simplified cryosytem possible with high temperature superconductor should make this goal attainable.

2. High field

As noted in sect. II.A above, in order to be in the radiation-dominated regime, the high field design must use magnets with fields of 12 T or above. The key to developing such magnets is the superconductor. This field range cannot be reached with NbTi technology; either Nb_3Sn @4^{o}K or a high temperature superconductor must be used. The latter possibility is very much the more attractive, as it offers the hope of a simple and low-cost cryogenic system.

Motivated by this possibility, a group at Brookhaven National Laboratory is proposing[6] a development program for a high-field, high-temperature (15-30^{o}K) superconducting tape wound magnet. The superconductor to be used is $YBa_2Cu_3O_7$, which has recently been shown[7] to be able to reach very high current densities at high fields, even at LN_2 temperatures. The goals of the program are:

• Development of superconducting tapes, with a thin (1-10 mm) film of epitaxial $YBa_2Cu_3O_7$, deposited on a biaxially aligned ZrO_2 buffer on a Ni-alloy substrate. The target performance is $J_C \sim 10^3 A/mm^2$ @ 10 T, 20^o K

• Characterization of the conductor (measurements of J_C, quench properties, mechanical properties, stability, etc.)

• Conceptual design of a tape-wound high-field magnet, including such issues as field quality and conductor placement, mechanical structure, quench properties, electrical behavior, and cryostat design. In this magnet, there will be many mechanical design challenges related to dealing with the large forces inevitable at high fields when using a conductor with not much strain tolerance. It is likely that the design will need to depart from the traditional cos θ coil arrangement.

It should also be noted that tape-wound coils will be susceptible to eddy currents which may limit the ac performance of the high field magnets.

B. Civil Construction/Installation/ Maintenance

1. High Field

Civil construction and maintenance in this case can proceed using conventional approaches. The relatively small diameter of the ring (2/3 that of the SSC), and consequently the "small" number of components, limits the cost of such activities.

2. Low field

In this case the large ring circumference implies substantial expenditures on the civil and installation efforts unless innovative, inexpensive tunneling, installation and maintenance technologies are used. Presently, the tunnel is foreseen to have a small (3-4 ft) diameter, with large distances between access shafts. The only large underground areas would be at the interaction points and at the straight sections where services like rf, injection and abort are required. The small diameter tunnel would be created using some form of "trenchless" technology. The possibilities include conventional tunnel boring machines, microtunnelling (either conventional or "enhanced"), or some form of horizontal drilling. The latter technique has been used over long distances but has limited accuracy.

Because a tunnel of this small a diameter would not be human-accessible, installation and maintenance of all components would be performed using robotics.

C. Cryogenics and Vacuum

1. High Field

I assume that the high field magnets will have a cold bore tube. If the magnets operate at 4^{o} K (e.g., for Nb_3Sn magnets), allowing the substantial amount of synchrotron radiation power to be deposited directly on the bore tube would put an enormous load on the cryogenic system. Hence, a beam screen will be required, operating at a temperature higher than 4^{o} K. Synchrotron radiation photons hitting the beam screen will desorb gases, principally H_2, CO and CH_4. These gases must be pumped by a distributed cryosorber, located between the beam screen and the magnet bore tube. To be an efficient H_2 pump, the cryosorber temperature must not be greater than 15-20^{o}K.

The use of high temperature superconducting magnets, operating in this temperature range, would allow the cryosorber to be integrated with the magnet bore tube. The cryogenic system would of course be much simpler in this case, with higher efficiency, simpler quench protection, and relaxed temperature regulation requirements.

2. Low field

The present concept of the low field magnets uses a warm bore aluminum beam pipe. A distributed pumping system (either ion pumps or getters) is integrated into the vacuum chamber (see fig. 3). The linear pumping speed needed to cope with the gas desorbed by synchrotron radiation[4] is similar to that required for the PEP II High Energy Ring.

The cryogenic distribution system in the tunnel is shown in fig 4. An example design for the required refrigeration system, in the case of a NbTi conductor at 4^{o}K, has been worked out [4]. The heat load would be about 0.2 W/m. For the 100 TeV/beam collider, 12 18 kW LHe refrigeration plants would be required, drawing 43 MW of wallplug power. A quench protection system for the 60 kA drive conductor could be constructed which would limit the peak temperature rise in a quench to <500^{o} K, and the peak voltage to <2000 v.

The use of a high temperature superconductor in the drive line would substantially reduce the size and cost of this cryogenic system. Operating costs would also drop dramatically. The wallplug power, for example, would drop to <5 MW if the drive line were operated at LN_2 temperature.

E. Abort/single point beam loss

As noted above in section III.B, both designs have attempted to limit the stored energy in the beam by using large bunch spacings. However, despite this, in the low field case, the large circumference still leads to very large values for the number of particles required, and hence to large beam stored energy. For the low field machine at 100 TeV/beam, the beams stored energy is 19 GJ. This amount of energy, even when dissipated uniformly in an iron abort dump 50 cm in diameter and 20 m long, will raise the iron temperature by 1400^{o} C. Abort design, and handling safely single-point beam loss events in the arcs, will be formidable problems.

F. Operations

Both the low field and the high field approaches are very large accelerators with complex operating scenario and very large part counts. Even with the substantial efforts being made to simplify components and to provide natural tolerance to errors, reliability will be a key issue. Design for reliability must be rigorously engineered into all components and subsystems from the very beginning if the final accelerator complex is expected to have a reasonable (>80%) availability.

V. CONCLUSION

In conclusion, table IX presents a list of the major issues common to both designs, and specific to the high and low field cases. At this workshop, one may hope that significant progress can be made in addressing many of these issues in the RLHC accelerator working group.

Table IX: List of major issues

Common to both	High field	Low field
Reliability	HTS conductor/ magnet development	Superferric/HTS magnet development
Interactions/crossing vs. bunch spacing	Method of longitudinal heating	Construction/ installation/ maintenance strategy
Aperture/cell length tradeoff	Vibration at interaction point	Single bunch/multibunch beam stability
Magnet field quality		Abort/single point beam loss
Interaction region optimization		Low frequency vibration/ripple sensitivity
Cryogenics/vacuum design		Emittance preservation
Injector optimization		

VI. REFERENCES

[1] *Proceedings of the Workshop on Future Hadron Facilities in the US*, (Bloomington, 1994), Fermilab TM-1907

[2] M. J. Syphers *et. al.*, "Beyond the LHC: A Conceptual Approach to a Future High Energy Hadron Collider", in *Proceedings of the 1995 Particle Accelerator Conference and International Conference on High Energy Accelerators* (Dallas, 1995), p. 431

[3] G. W. Foster, E. Malamud, "Low-cost Hadron Colliders at Fermilab", Fermilab TM-1976 (1996)

[4] "New Low-Cost Approaches to High Energy Hadron Colliders at Fermilab", mini-symposium at the spring APS meeting, Indianapolis (1996)

[5] S. Peggs *et. al.*, "Lattice Optimization for a Really Large Hadron Collider(RLHC)", submitted to the European Particle Accelerator Conference (1996)

[6] M. Harrison *et. al.*, "A Proposal to Conduct an Investigation into the Feasibility of the Use of High T_c Materials for Superconducting Accelerator Magnets of the kind needed for Next Generation Accelerators", Brookhaven (1996) (unpublished)

[7] D. Wu *et. al.*, Appl. Phys. Lett. **67**, 2397 (1995)